MINUTIAE DATA SYNTHESIS FOR FINGERPRINT IDENTIFICATION APPLICATIONS

Kar-Ann Toh, Wei-Yun Yau, Xudong Jiang, Tai-Pang Chen, Juwei Lu and Eyung Lim
Centre for Signal Processing
School of Electrical & Electronic Engineering
Nanyang Technological University, Singapore
Email: ekatoh@ntu.edu.sg

ABSTRACT

In this paper, we address the false rejection problem due to small solid state sensor area available for fingerprint image capture. We propose a minutiae data synthesis approach to circumvent this problem. Main advantages of this approach over existing image mosaicing approach include low memory storage requirement and low computational complexity. Moreover, possible matching search overhead due to data redundancy could be reduced. Extensive experiments were conducted to determine the best transformation suitable for minutiae alignment. Among the three transformations presented, affine transformation is found to be most suited for minutiae alignment. We demonstrate the idea of synthesis with an example using physical fingerprint images. The proposed synthesis system is also shown to reduce the number of false rejects caused by the use of different fingerprint regions for matching.

1. INTRODUCTION

In general, an automatic fingerprint identification or verification (see e.g. [1, 2, 3, 4]) system consists of three main processing stages namely, image acquisition, feature extraction and matching. In image acquisition, query and template database images are acquired through various input devices. Development over the years has seen through means that mechanically scan the ink based fingerprints into the computer system, to means which directly capture the fingerprints using sophisticated solid state sensors. With fingerprint images which could be distorted or contaminated with noise, the automated system seeks to extract characteristic features which are discriminating for different fingers and yet invariant with respect to image orientation for same fingers. The final stage of fingerprint identification or verification is to search and verify matching image pairs.

The use of ink-less sensors has advanced the data acquisition aspects in an automatic fingerprint identification or verification system. This includes optical and solid state devices. By means of CCD array and laser technologies, the optical sensors offer a cost effective solution for fingerprint image capture. Conforming to the regulation by National Institute of Standard and Technology (NIST, USA), conventional optical sensors have a sensing area of 1-inch by 1-inch. As for solid state sensors, which adopt capacitance, electric field, pressure or temperature sensing technologies, they offer compact means for fingerprint image capture with features to detect presence of fingers such as locally adjustable automatic gain control [5]. However, due to manufacturing limitation and cost factors, most solid state sensors do not come with large sensing area (e.g. Veridicom's *i*Touch has a sensing area of 1.5cm by 1.5cm and Infineon's FingerTip has a sensing area of 11.1mm by 14.3mm). Moreover, the imaging area for the finger is further restricted to the area in contact with the sensor. This, as compared to conventional ink based rolled fingerprint impression, possesses a much smaller information area. A consequence of this can be seen in using different partial areas of the same finger for matching, which causes false rejection. For this reason, during enrollment of a person in a database, a rolled fingerprint would be preferred over a plain touch impression.

Apart from requiring the individual user to ensure good placement of fingerprint area during image acquisition process, few automatic fingerprint identification/verification system has addressed the problem of false rejection cause by using different image regions for matching. While acquiring a few separate fingerprint images during registration could simply handle the false reject problem, much of the acquired information could be redundant (due to much common regions) and hence takes up unnecessarily large storage space. Moreover, overheads of the multimodal search would increase due to the much larger number of records available for matching. In [6], an image mosaicing technique is developed for constructing a rolled fingerprint from an image sequence of partial fingerprints. The proposed fingerprint mosaicing algorithm consists of four stages namely, (i) segmentation of foreground and background areas in each frame; (ii) weighting of each image's contribution using a foreground mask; (iii) stacking of the weighted gray scale frames to compute the mosaic gray scale image; (iv) stacking of the foreground masks to compute a confidence index at every pixel. Although mosaicing technique possesses the capability of acquiring a larger area of fingerprint image, it is at the expense of larger sensor area for rolling as well as larger storage requirement for a much larger synthesized image. Moreover, as seen from the pixel level computation which is applied directly to the acquired image, the computational cost is high.

In this paper, we propose a minutiae based synthesis method for an automatic fingerprint identification/verification system. The proposed methodology not only synthesize necessary information for fingerprint identification, but also possesses several desired features: (i) no restriction on the hardware sensor area; (ii) small storage requirement since the synthesized data contains only the necessary minutiae information needed for matching. This is especially useful for search within a large database in fingerprint identification; and (iii) low computational complexity for the synthesis algorithm.

2. MINUTIAE DATA SYNTHESIS

Our representation for the fingerprint consists of a global structure and a local structure [7]. The global structure consists of positional and directional information of ridge endings and ridge bifurcations. The local structure consists of relative information of each detected minutia with other neighboring minutiae. Since the local structure contains relative information which is insensitive to rotation and translation, the main issue concerning minutiae data synthesis is to establish the relationship between the global structures of two fingerprints acquired with common regions.

Let

$$M = \{(x_i, y_i, \varphi_i, t_i)\},\ i = 1, 2, ...n \qquad (1)$$

be the set of minutiae containing the positional information (x, y), directional information (φ) and minutiae type information ($t_i =$

0-7803-6725-1/01/$10.00 ©2001 IEEE

0 indicates a ridge ending and $t_i = 1$ indicates a bifurcation) for n minutiae elements in the global structure.

Suppose we have a total of m number of minutiae data sets from m partial fingerprints of a same finger, then we can write for the k^{th} minutiae data set as:

$$M_k = \{(x_i, y_i, \varphi_i, t_i)\}_k,\ i = 1, 2, ...n_k,\ k = 1, 2, ..., m. \quad (2)$$

Among these minutiae data sets, there would be common regions whereby information is redundant. If it is to search through each individual minutiae data sets for matching, it would not be cost effective since these redundant information are being searched through more than once. Moreover, the geometrical relationships among these minutiae data sets are no longer preserved since these data sets are treated as separate entity. In order to save data storage space with respect to redundancy as well as to provide a good overall picture about the minutiae sets, a synthesis with consideration to relationship between data sets is needed.

For fingerprint images with common regions, we can express the resultant synthesized information as:

$$M_{\cup_1^m} = \bigcup_{k=1}^{m} \{f_k(x_i, y_i, \varphi_i, t_i)\}_k,\ i = 1, 2, ...n_k \quad (3)$$

where $f_k,\ k = 1, 2, ..., m$ denote the necessary topological transformations for aligning the different sets of minutiae data. Suppose o_1 is the number of overlapping points between M_1 and M_2. Then the number of minutiae points in $M_{\cup_1^2}$ can be expressed as $n(M_{\cup_1^2}) = n_1 + n_2 - o_1$. Now let o_2 be the number of overlapping points between $M_{\cup_1^2}$ and M_3. And the number of minutiae points in $M_{\cup_1^3}$ is $n(M_{\cup_1^3}) = n_1 + n_2 + n_3 - o_1 - o_2$. In short, the total number of minutiae points in the synthesized minutiae data set $M_{\cup_1^m}$ can be written as:

$$n(M_{\cup_1^m}) = \sum_{k=1}^{m} n_k - \sum_{k=1}^{m-1} o_k, \quad (4)$$

where o_k is the number of overlapping minutiae points between $M_{\cup_1^k}$ and M_{k+1}. Hence, if each o_k is of considerable size, the total number of minutiae in the synthesized data set $(n(M_{\cup_1^m}))$ can be significantly smaller than $\sum_{k=1}^{m} n_k$.

Upon acquiring two images for synthesis, the task immediately after minutiae detection is to find correspondence between these two images so that the global minutiae information between the two images can be aligned. We shall discuss our alignment method in a separate section.

Let M_j and M_k, $j \neq k$, $j, k \in \{1, 2, ..., m\}$, be two fingerprint minutiae data sets to be synthesized. Suppose there are p corresponding points (minutiae coordinates) between the two images. Denote this set of p corresponding points by C. Then, a topological transformation f can be determined relating M_j and M_k from $\mathbf{x}_j = f(\mathbf{x}_k)$ where $\mathbf{x}_j = \{(x_i, y_i)\}_j$ and $\mathbf{x}_k = \{(x_i, y_i)\}_k$ for all $i \in C$. Since the transformation will be used for aligning those non-corresponding minutiae points, a careful study on its sensitivity with respect to noise and deformation is necessary. We shall discuss various transformation models for image points alignment right after the following section.

3. MINUTIAE DETECTION AND ALIGNMENT

For minutiae detection, we adopt an adaptive ridge tracing algorithm which is evolved from [8]. Our approach adaptively traces the gray-level ridges of the fingerprint image and applies adaptive oriented filters to the image only at those regions that require to be smoothed. A long tracing line will be obtained when there is little variation in contrast and when the bending level of the ridge is low. Main advantage of our approach is that tracing is by adaptive piece wise linear approximation of the ridges which speeds up the process of ridge detection as compared to other methods which adopt either pixel wise or fixed step tracing [9]. The tracing is only performed within the region of interest. The region of interest is segmented based on the local certainty level $c(x, y)$ at pixel (x, y) on image $\mathbf{I}$.

Having the minutiae extracted for two images, it is necessary to align the two sets of data so that they form a larger picture of the fingerprint. Problems which are inherent to this alignment process include: (i) translation and rotation variance between the two fingerprint images; (ii) deformation of the fingerprint images which induces location errors.

Together with an indication of ridge ending and ridge bifurcation, the notation in (1) provides a global description of the minutia. Since this feature vector is not rotation and translation invariant, we use a local feature vector for the alignment purpose. Let m_j, $j = 1, 2, ..., l$ be the j^{th} nearest neighbour with respect to m_0. Denote the distance between m_0 and m_j by d_{j0} and the relative radial angle for m_j with respect to m_0 by θ_{j0}. Let c_{j0}, $j = 1, 2, ..., l$ be the ridge count between m_0 and m_j, then together with corresponding minutiae type t_{j0} the local feature vector is packed as $F_{lj} = [d_{j0}, \theta_{j0}, c_{j0}, t_{j0}]^T,\ j = 1, 2, ..., l$. It is obvious that this local structure is rotation and translation invariant since it contains only relative information. Hence, it can be used directly for preliminary local alignment matching. A match weighting the similarity between the local feature vectors from the two images is performed so that a common reference can be established. The reader is referred to [7] for greater details on these local and global structures and the corresponding matching.

Once the preliminary correspondence between these local features is established, the transformation required for global alignment can be found. To validate good correspondences for this transformation, a further match combining both local and global information is adopted. We shall discuss such transformation for image points alignment in the following section.

4. TRANSFORMATIONS FOR ALIGNMENT

Consider two sets of image points: $\mathbf{x} = (x, y)$ and $\mathbf{X} = (X, Y)$. The problem here is to find the best transformation f that relates these two sets of image points, i.e. $\mathbf{x} = f(\mathbf{X})$. For linear transformations, we have $\mathbf{x} = \mathbf{TX}$ where $\mathbf{T}$ denotes the transformation matrix. In the following, we examine different transformation models for our fingerprint data synthesis application.

4.1. Affine transformation

Affine geometry compares distances only on the same line or on parallel lines. As compared to the Euclidean geometry, affine geometry relaxes the requirement on perpendicularity. Hence transformation under affine geometry is more general as compared to that under Euclidean geometry. An affine transformation $\mathbf{T}$ relating $\mathbf{x}$ and $\mathbf{X}$ can be written as:

$$\begin{bmatrix} x \\ y \end{bmatrix} = \begin{bmatrix} t_{11} & t_{12} & t_{13} \\ t_{21} & t_{22} & t_{23} \end{bmatrix} \begin{bmatrix} X \\ Y \\ 1 \end{bmatrix} \quad (5)$$

where the six unknown transformation parameters $(t_{ij},\ i = 1, 2;\ j = 1, 2, 3)$ can be solved using at least three pairs of non-collinear corresponding image points (x, y) and (X, Y).

4.2. Projective transformation

Projective geometry is the result of relaxing the restrictions preserving parallel lines but require that straight lines remain straight

lines for any changes we might impose on the figure. In homogenous coordinates, projective transformation can be written as:

$$\begin{bmatrix} x_1 \\ x_2 \\ x_3 \end{bmatrix} = \begin{bmatrix} t_{11} & t_{12} & t_{13} \\ t_{21} & t_{22} & t_{23} \\ t_{31} & t_{32} & 1 \end{bmatrix} \begin{bmatrix} X \\ Y \\ 1 \end{bmatrix}, \quad (6)$$

for which

$$x = \frac{x_1}{x_3} = \frac{t_{11}X + t_{12}Y + t_{13}}{t_{31}X + t_{32}Y + 1}, \quad y = \frac{x_2}{x_3} = \frac{t_{21}X + t_{22}Y + t_{23}}{t_{31}X + t_{32}Y + 1}. \quad (7)$$

For each point on the image plane, one can form two equations using x and y from and (7):

$$t_{11}X + t_{12}Y + t_{13} - t_{31}xX - t_{32}xY = x, \quad (8)$$

$$t_{21}X + t_{22}Y + t_{23} - t_{31}yX - t_{32}yY = y. \quad (9)$$

The eight unknowns can be solved using at least 4 corresponding points from the image data.

4.3. Topological transformation

Topology encompasses the projective, affine and Euclidean geometries. An even smaller set of properties is invariant under topological transformation (e.g. preserving only closed curves, order and connectivity). In this study, only the quadratic type of topological transformation is investigated. The following transformation presents one quadratic transformation without interaction between the orthogonal coordinates.

$$\hat{x} = t_1X + t_2Y + t_3 + t_7X^2 + t_8Y^2, \quad (10)$$

$$\hat{y} = t_4X + t_5Y + t_6 + t_9X^2 + t_{10}Y^2. \quad (11)$$

Minimization objective and solution:

For topological (nonlinear) transformation setup as above, the following least squares minimization objective can be used to solve for the unknown transformation parameters:

$$f = \sum_i \left[(x_i - \hat{x})^2 + (y_i - \hat{y})^2\right], \quad (12)$$

where x_i and y_i are the measured image point coordinates.

Packing (10) and (11) in matrix form, we can write for each image data point, $\mathbf{Ab} = \mathbf{c}$, where

$$\mathbf{A} = \begin{bmatrix} X & Y & 1 & 0 & 0 & 0 & X^2 & Y^2 & 0 & 0 \\ 0 & 0 & 0 & X & Y & 1 & 0 & 0 & X^2 & Y^2 \end{bmatrix}$$

$$\mathbf{b} = [t_1\ t_2\ t_3\ t_4\ t_5\ t_6\ t_7\ t_8\ t_9\ t_{10}]^T, \quad \mathbf{c} = [x\ y]^T. \quad (13)$$

The solution to the least squares minimization objective (12) is the parameter vector $\mathbf{b}$ satisfying the normal equation $\mathbf{A}^T\mathbf{Ab} = \mathbf{A}^T\mathbf{c}$ where $\mathbf{A}$, $\mathbf{b}$ and $\mathbf{c}$ are stacked according to multiple data points.

5. EXPERIMENTS

5.1. Transformation study

In this section, we perform experimental study, using physical fingerprint data, to determine the best transformation for minutiae synthesis. We collect 5 images corresponding to 5 different areas (centre, top-left, top-right, bottom-left and bottom-right) for each finger for the experiment. A total of 200 images were captured using the Veridicom Sensor for 40 fingers.

Matching was first performed to obtain the corresponding coordinates between two images which are to be synthesized. We used the centre area as the base image to match with one of the other areas (top-left, top-right, bottom-left and bottom-right) of the same finger. The matched image pairs with 10 or more corresponding minutiae coordinates were then used for the following transformation study. As a result, only 50 matched pairs were found to have 10 or more matched points.

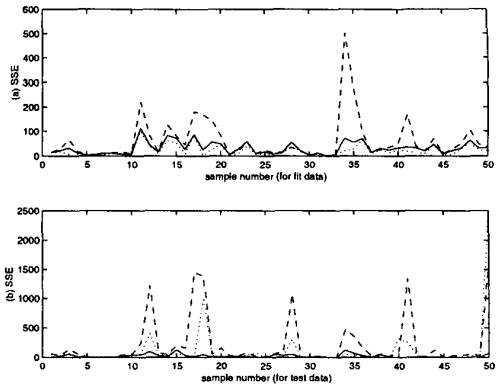

Fig. 1. (a) and (b) Sum of squared error distribution for fit and test data

Table 1. Sum of Squared Errors for fit and test data

Sum of squared error for fit data			
	Affine	Projective	Nonlinear
Mean	31.1304	62.2254	16.4531
STD	25.3905	87.7418	19.4167
Sum of squared error for test data			
	Affine	Projective	Nonlinear
Mean	28.2344	227.7379	464.9472
STD	29.7245	428.2317	1559.9000

To assess the accuracy of each transformation discussed in previous section, 3/4 of the matched points were used for identifying the transformation parameters (fitting) and the rest of 1/4 were used for extrapolation test (testing). The distribution of the sum of squared errors (SSE) for these matched pairs are plotted in Fig. 1(a) and Fig. 1(b) for fit data and test data respectively. The continuous line ('___') corresponds to SSE distribution for affine transformation. The dashed line ('- -') and the dotted line ('...') correspond to projective transformation and topological transformation respectively. The mean value and the standard deviation (STD) for these errors are also tabulated in Table 1 to reflect an overall view of these results.

As seen from Fig. 1(a), the topological (quadratic) transformation provides the best fit since the dotted curve falls below the other two curves for all samples. This is also reflected in Table 1 since the mean SSE and the standard deviation (STD) are the smallest among the three transformations. Here we note that the projective transformation, being sensitive to the matrix inversion, shows rather poor results as compared to that of affine transformation. As for test data not included in the fitting process, results from Fig. 1(b) and Table 1 show that affine transformation gives the best result, in the sense of lowest mean SSE and lowest STD. It is important to note that both the mean SSE and STD for the other two transformations (projective and topological) are considerably huge as compared to those by affine transformation. Main reason being that coordinate warping according to the fit data (interpolation) may not necessary fit well the test data (extrapolation). Base on this study, the affine transformation is adopted for alignment in our minutiae synthesis system.

5.2. A minutiae synthesis example

In this part, we show an example of synthesizing three fingerprint images. As shown in Fig. 2(a) through Fig. 2(c), three fingerprint images are captured from three different portions of the same fin-

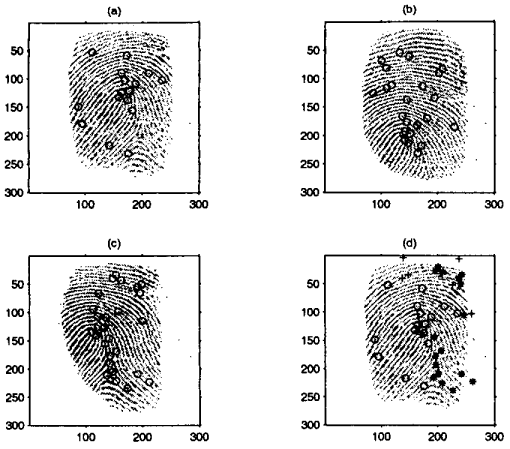

Fig. 2. Fingerprint samples with detected minutiae

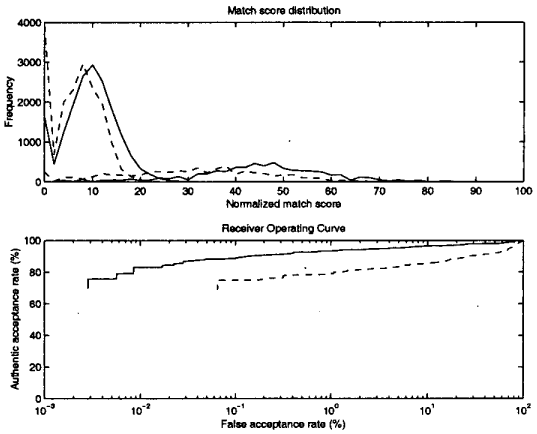

Fig. 3. Frequency and ROC curves

ger using Veridicom's *i*Touch sensor. Minutiae points (shown in circles in Fig. 2(a)-2(c)) are detected from these fingerprint images using the ridge tracing algorithm. A visual examination on these figures shall reveal that the minutiae information extracted in each image contains similar points (found in common regions) and dissimilar points (found outside common regions). It is also observed that even within the common region, some minutiae detected in one image may not be detected in another image due to different image qualities. Due to these reasons, when any two of these three images are used for matching in a fingerprint identification or verification system, false rejection would occur when the threshold related to the total number of matched minutiae from the query image is set rather high.

Fig. 2(d) shows the synthesized minutiae points from Fig. 2(a)-2(c)) using Fig. 2(a) as the background image. The 'circles' in the figure indicates the original detected minutiae points from Fig. 2(a), whereas the 'plus' and 'stars' indicate those additional minutiae points transferred from Fig. 2(b) and Fig. 2(c) respectively. As seen from this figure, these additional minutiae points have found correct correspondences on the fingerprint image (Fig. 2(a)) which are not detected in the original capture. A match comparing a query image data with minutiae data from Fig. 2(d) will have a higher matching count.

5.3. Performance evaluation

In this experiment, we show that the fingerprint synthesis method can improve performance in terms of False Rejection caused by using different regions of fingerprints for matching. A test sample consisting of 600 query images and 2 × 60 template data sets (set(a) and set(b)) were used for this matching evaluation. All images were captured using Veridicom's *i*Touch sensor. The query images were randomly acquired from different partial regions (some of these are very much towards the edge) of each finger. Set(a) template data were obtained from the central region of each finger and set(b) template data were obtained from synthesizing five different regions of each finger.

Scoring results in terms of the frequency plots and ROC plots are shown in Fig. 3 for 36000 matchings. The dashed curves and the continuous curves represent matching results using set(a) templates and set(b) templates respectively. Due to the use of different partial fingerprint regions for matching, results obtained from using set(a) templates are rather poor as seen from the figure. The situation has been significantly improved by using set(b) templates for matching. Notice that by using the syhthesized templates, both matching curves for the same fingers (curves on the right) and those for different fingers (curves on the left) in the frequency plots show a shift of scores towards the higher region. However, this does not show deterioation of performance in terms of false acceptance rate. In fact it shows improvement of matching performance as seen from the ROC curves.

6. CONCLUSION

In view of the limitation in solid state image sensor area, we propose, in this paper, a method to synthesize fingerprint data for data acquisition enhancement. The method is advantages over existing mosaicing technique in terms of low computational cost and low memory storage requirements. Several transformation models were compared for minutiae points alignment. The affine transformation, which was found to provide good interpolation and extrapolation capabilities, was adopted for minutiae data synthesis. The synthesized template data set was found to improve matching performance in the sense of reducing false rejection caused by using different fingerprint regions from the same finger for matching.

7. REFERENCES

[1] Anil Jain, Lin Hong, and Ruud Bolle, "On-line fingerprint verification," IEEE Trans. Pattern Analysis and Machine Intelligence, vol. 19, no. 4, pp. 302–313, 1997.

[2] Anil K. Jain, Lin Hong, Sharath Pankanti, and Ruud Bolle, "An identity-authentication system using fingerprints," in Proceedings of the IEEE, 1997, pp. 1365–1388.

[3] Nalini K. Ratha, Kalle Karu, Shaoyun Chen, and Anil K. Jain, "A real-time matching system for large fingerprint databases," IEEE Trans. Pattern Analysis and Machine Intelligence, vol. 18, no. 8, pp. 799–812, 1996.

[4] U. Halici, L. C. Jain, and A. Erol, "Introduction to fingerprint recognition," in Intelligent Biometric Techniques in Fingerprint and Face Recognition, L. C. Jain and et. al., Eds., pp. 3–34. The CRC Press international series on computational intelligence, 1999.

[5] Lawrence O'Gorman, "Fingerprint verification," in Biometrics: Personal Identification in Networked Society, Anil K. Jain, Ruud Bolle, and Sharath Pankanti, Eds., 1999, pp. 43–64.

[6] Nalini K. Ratha, Jonathan H. Connell, and Ruud M. Bolle, "Image mosaicing for rolled fingerprint construction," in 14th International Conference on Pattern Recognition, 1998, vol. 2, pp. 1651–1653.

[7] Xudong Jiang and Wei Yun Yau, "Fingerprint minutiae matching based on the local and global structures," in 15th Internaional Conference on Pattern Recognition, 2000, vol. 2, pp. 1042–1045.

[8] D. Maio and D. Maltoni, "Direct gray-scale minutiae detection in fingerprints," IEEE Trans. Pattern Analysis and Machine Intelligence, vol. 19, no. 1, pp. 27–40, 1997.

[9] Xudong Jiang, Wei Yun Yau, and Wee Ser, "Minutiae extraction by adaptive tracing the gray level ridge of the fingerprint image," in IEEE Internaional Conference on Image Processing (ICIP'99), 1999, vol. 2, pp. 852–856.